

INTERSTELLAR COMMUNICATION. III. OPTIMAL FREQUENCY TO MAXIMIZE DATA RATE

MICHAEL HIPPKE¹ AND DUNCAN H. FORGAN^{2,3}¹ Sonneberg Observatory, Sternwartestr. 32, 96515 Sonneberg, Germany² SUPA, School of Physics & Astronomy, University of St Andrews, North Haugh, St Andrews, Scotland, KY16 9SS, UK³ St Andrews Centre for Exoplanet Science, University of St Andrews, UK

ABSTRACT

The optimal frequency for interstellar communication, using “Earth 2017” technology, was derived in papers I and II of this series (Hippke 2017a,b). The framework included models for the loss of photons from diffraction (free space), interstellar extinction, and atmospheric transmission. A major limit of current technology is the focusing of wavelengths $\lambda < 300$ nm (UV). When this technological constraint is dropped, a physical bound is found at $\lambda \approx 1$ nm ($E \approx$ keV) for distances out to kpc. While shorter wavelengths may produce tighter beams and thus higher data rates, the physical limit comes from surface roughness of focusing devices at the atomic level. This limit can be surpassed by beam-forming with electromagnetic fields, e.g. using a free electron laser, but such methods are not energetically competitive. Current lasers are not yet cost efficient at nm wavelengths, with a gap of two orders of magnitude, but future technological progress may converge on the physical optimum. We recommend expanding SETI efforts towards targeted (at us) monochromatic (or narrow band) X-ray emission at 0.5–2 keV energies.

1. INTRODUCTION

The idea to communicate with Extraterrestrial Intelligence was born in the 19th century. The first known proposal was made by the mathematician Carl Friedrich Gauß who suggested to cut a giant triangle in the Siberian forest and plant wheat inside. His motivation was that “a correspondence with the inhabitants of the moon could only be begun by means of such mathematical contemplations and ideas, which we and they have in common.” (Crowe 1999). Such a passively displayed message could be reinforced following an idea by Joseph von Littrow, who suggested in the 1830s to dig trenches in the Sahara desert, again in precise geometric shapes, and fill these with kerosene; lit at night they would signal our presence (Van Tran 1992).

Humans also looked for similar features on other planets. The late 19th century was a time when many great canals were built on earth, such as the Suez Canal (1869) and the Panama Canal (start in 1880). Naturally, it was thought that similar projects would be undertaken by other advanced civilizations as well, and Schiaparelli (1878) announced the discovery of “canali” on Mars, confirmed by Lowell (1904).

It was not long after the invention of the radio by Marconi (1897) when Nikola Tesla (1901) searched for radio signals, and detected coherent signals which he

believed to originate from intelligent beings on Mars. In the optical, William Pickering (1909) suggested to send a Morse code to Mars using reflected sunlight with gigantic mirrors.

Today, we are amused about these naïve attempts. Yet, it is enlightening to reflect on the thoughts which Phil Morrison had when writing his seminal paper on radio SETI (Cocconi & Morrison 1959): “And Cocconi came to me one day – I’ve often reported this – and said, ‘You know what, Phil? If there are people out there, won’t they communicate with gamma rays that’ll cross the whole galaxy?’ And I said, ‘Gee, I know nothing about that (...) Why not use radio? It’s much cheaper. You get many more photons per watt and that must be what counts.’ And we began working on that and pretty soon we knew enough about radio astronomy to publish a paper called, ‘Searching for Interstellar Communications.’” (Gingerich 2003).

Morrison’s statement of radio being superior is correct for the case where no tight directivity is needed, such as an omni-directional beacon. For constant power, constant detector efficiency per photon, and negligible extinction, the number of photons at the receiver is maximized for lower-energy photons. Thus, microwaves work well for an interstellar lighthouse. However, in their paper they discuss the directed communication between two nearby (10 LY) civilizations, and the authors are well aware of the weak focusing for radio waves, because they hope for larger (200 m class) dishes in the future. They also seek to maximize the data rate, but strug-

gle in their bandwidth analysis: The correct framework for the photon-limited communication capacity was only recently completed by Holevo (1973) and Giovannetti et al. (2004a, 2014) as discussed in detail in the first paper in this series (Hippke 2017a). Morrison’s reason to disfavor optical and γ -ray communication was that they “demand very complicated techniques”, a correct assessment in the 1950s.

Incidentally, only months later, optical communication became feasible with the discovery of the laser by Maiman (1960). It was quickly realized that the tighter beam of optical communication can increase the data rate compared to radio (Schwartz & Townes 1961); the authors noted the rapid development: “No such device was known a year ago”.

To sum up, the evolution of interplanetary/interstellar communication technology migrated from planting trees, burning kerosene, reflecting sunlight, to sending electromagnetic waves in the radio, microwave and optical. Every technological step was driven by the availability of new technology, consistently considered to be the best option possible. But what if each one is an observational bias, comparable to the streetlight effect¹: people are searching for something and look only where it is easiest?

Because of the fast technological changes, we should not focus on the “sweet spot” of our time, but instead derive the physical optimum. More advanced civilizations can be assumed to have developed the technology for such optimal communication.

2. OPTIMAL FREQUENCY

In this paper, we restrict ourselves to photons as information carriers and neglect other particles such as neutrinos or protons, as well as exotic methods such as gravitational waves, occulters or inscribed matter. These other options will be treated in another paper of the series.

We will now derive the optimum photon communication frequency within the laws of physics. The quest is as follows: Assume a civilization has two distant (e.g. $d = 1.3$ pc) locations that wish to communicate with each other. Both know of each others existence and position, they operate circular apertures as transmitter D_t and receiver D_r , and they strive to maximize the number of bits exchanged (per unit time, DR) for some power P_t which might be large, but finite. Interstellar extinction between the two stations (S_E) has been measured per frequency, and both stations are in space with no atmo-

¹ A policeman sees a drunk man searching for something under a streetlight, and asks what he has lost. He says he lost his keys and they both look under the streetlight together. After a few minutes the policeman asks if he is sure he lost them here, and the drunk replies, “no”, and that he lost them in the park. The policeman asks why he is searching here, and the drunk replies, “this is where the light is”.

spheric losses, $S_A = 1$. Using the framework derived in Hippke (2017a), we can calculate the data rate (in bits per second) as

$$DR = \frac{S_E P_t D_t^2 D_r^2}{4 h f Q^2 \lambda^2 d^2} \times g(\eta M + (1 - \eta) N_M) - g((1 - \eta) N_M) \quad (1)$$

where the first term has the number of photons received (per second if P is in Watt), h is Planck’s constant ($\approx 6.626 \times 10^{-34}$ J s) and $Q \approx 1.22$ is the diffraction limit for a circular transmitting telescope (Rayleigh 1879) of frequency $f = 1/\lambda$.

The second term is the Holevo capacity (in bits per photon), where η is the receiver efficiency and $g(x) = (1 + x) \log_2(1 + x) - x \log_2 x$ so that $g(x)$ is a function of $\eta \times M$. M is the number of photons per mode, and N_M is the average number of noise photons per mode (Giovannetti et al. 2014).

While extinction is a function of wavelength and distance, we can neglect its influence for wavelengths far from the Lyman continuum (91.2 nm, Figure 1) for short (pc) distances, because it is of order unity.

Equally, capacity (in bits per photon) is a function of wavelength, because N_M (the number of noise photons per mode) depends on the number of modes M , and on wavelength-dependent background flux. While astrophysical noise varies over several orders of magnitude by wavelength, capacity follows a logarithmic relation so that the impact is only a factor of a few as long as the flux is larger than the noise.

To build some intuition before entering a detailed discussion, we set power, distance, aperture, S_E , M and N_M as constant. Then, eq. 1 scales as

$$DR \propto f Q \quad (2)$$

so that higher frequencies have a positive linear relation for higher data rates. Photon energy depends on wavelength, $E = hc/\lambda$, which makes higher frequency photons more costly in terms of energy. Yet, the beam angle decreases linearly for higher frequencies, and thus the flux decreases quadratically for the area in the beam. The overall effect is a positive linear function so that higher frequencies allow for more photons in the receiver, all other things equal.

The factor Q imposes a limit due to the mechanical quality of the machine. As we will see in section 2.1, there is a physical limit to Q for high frequencies (small wavelengths) because mirror smoothness is limited to atomic sizes, and focusing with electromagnetic fields is inefficient (section 2.3).

2.1. Focusing: limits from surface roughness

For diffraction-limited telescope mirrors or lenses, the polished surface needs to have a smoothness smaller

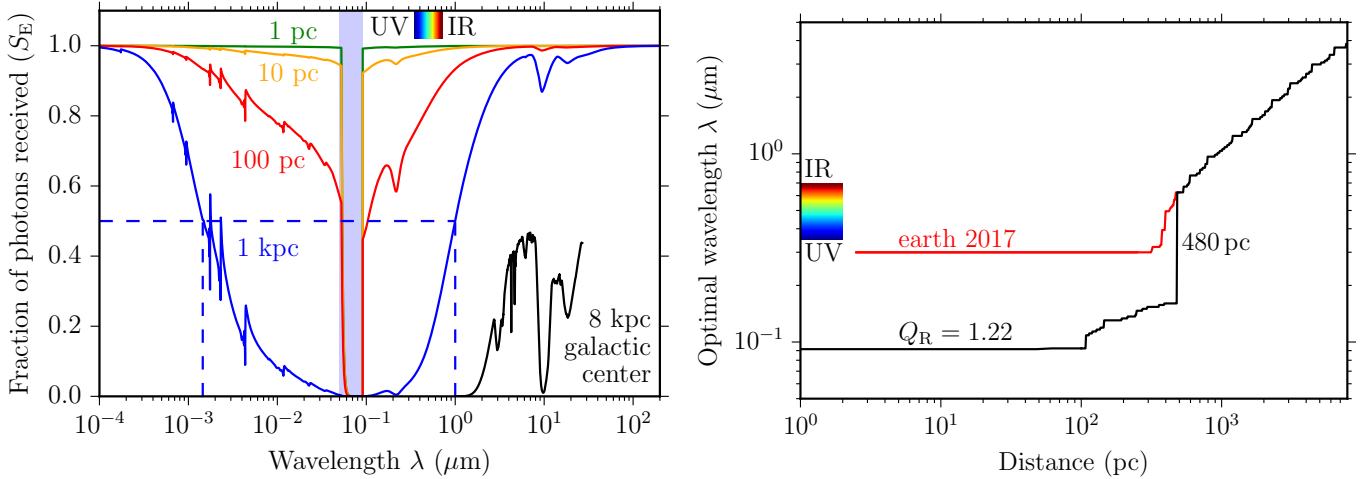


Figure 1. Left: Fraction of photons that defies interstellar extinction (S_E), as a function of wavelength λ , shown for different distances. The dashed blue line shows 50% extinction for the 1 kpc distance which occurs for $\lambda = 1 \mu\text{m}$ and $\lambda = 0.5 \text{ nm}$ on both sides of the Lyman continuum ($\lambda \approx 50 \dots 91.2 \text{ nm}$) which is opaque even for the closest stars due to the ionization of neutral hydrogen (Aller 1959; Wilms et al. 2000; Barstow & Holberg 2007). Right: Optimal wavelength for communication as a function of distance, shown for the case of low-energy photon communication ($\lambda > 91.2 \text{ nm}$). Current technology (red line) is only diffraction-limited down to $\lambda \gtrsim 300 \text{ nm}$, while the physical limit (black line) favors wavelengths close to the Lyman limit.

than the wavelength (Rayleigh 1879; Danjon & Couder 1935). Precisely, a perfect surface would concentrate 84% of the light into the central Airy Disk, and the remains into the diffraction rings. A “good” optical surface is typically assigned to a Strehl value of 80% (Strehl 1894), resulting in 64% of the flux inside the Airy Disk, and requiring $< \lambda/4$ peak-to-valley (pv) as well as $< \lambda/14$ root-mean-square (rms) surface accuracy (Smith 2008).

This accuracy is trivially possible at microwave frequencies, e.g. 1.4 GHz corresponds to $\lambda \approx 21.4 \text{ cm}$, so that $\lambda/14 \approx 1.5 \text{ cm}$, surpassed by any metal dish. Parabolic optical ($\lambda = 400 \dots 700 \text{ nm}$) mirrors are regularly polished to $< 100 \text{ nm}$ accuracy by amateurs using hand tools (Texereau 1984). The physical limit for any material is set by the atomic radius of order 0.1 nm (Bohr 1913). Theoretical X-Ray focusing limits stem from the fact that X-rays are scattered at the electrons of the atomic shell (Kirkpatrick & Baez 1948; Suzuki 2004). Resulting limits have been calculated for many materials such as Be (0.028 nm) and Os (0.034 nm) (Yu et al. 1999). The best suited material appears to be the one with the highest density which can be used to fabricate a reflector, and is currently believed to be osmium ($\rho = 22.57$) (Suzuki 2004).

In practice, mirrors with a surface quality at this level have been produced (Yamamoto 2001; Tsuru et al. 2009). For example, the mirror of the “Coherent X-ray Imaging instrument” has been measured with a surface roughness of 0.57 nm (rms) and 2.5 nm pv (Siewert et al. 2012). The X-ray mirror of the XFEL instrument is specified as 0.25–0.5 nm rms (Bean et al. 2016). The mirrors of the Chandra space telescope were polished

to 0.185–0.344 nm rms, close to the size of one Ir atom ($r=0.135 \text{ nm}$) (Weisskopf 2012).

Taking a surface roughness of 0.2 nm rms results in a 80% Strehl ratio for $\lambda > 2.8 \text{ nm}$. The theoretical physical limit allows for “good” optics for $\lambda > 0.48 \text{ nm}$ using Osmium. This limit could hypothetically be extended using degenerate matter (e.g. from Neutron stars) where the electrons are compressed more tightly, but it is unclear if such a fabrication is possible, so that it is neglected here. We will instead adopt a minimum wavelength of order $\lambda = 1 \text{ nm}$ as the plausible physical limit, a factor of two added to the hard cut, because a reflective coating at these wavelengths will likely not be possible with the densest material (Osmium), as discussed in the following section.

2.2. Reflectivity at nm wavelengths

Classical parabolic mirrors at these wavelengths suffer from low reflectivity, because the refractive index of most materials converges to unity at high (keV, $\lambda \approx \text{nm}$) energies. This makes it difficult to focus photons efficiently and avoid absorption (Aristov & Shabel’nikov 2008), and it makes lenses impossible with known materials. Current limits at $\lambda = 11 \text{ nm}$ (extreme ultraviolet, EUV) and normal (not grazing) incidence angle are 80% reflectivity using exotic alloys (Singh & Braat 2000). For shorter wavelengths (X-rays, below 5 nm/250 eV), grazing incidence mirrors (at angles of a few degrees) are common. Their disadvantage are long focal lengths and/or the need for multiple mirrors. However, technological progress in material sciences is rapid and order unity reflectivity for nm wavelengths at normal incidence angles might be feasible with yet unknown alloys.

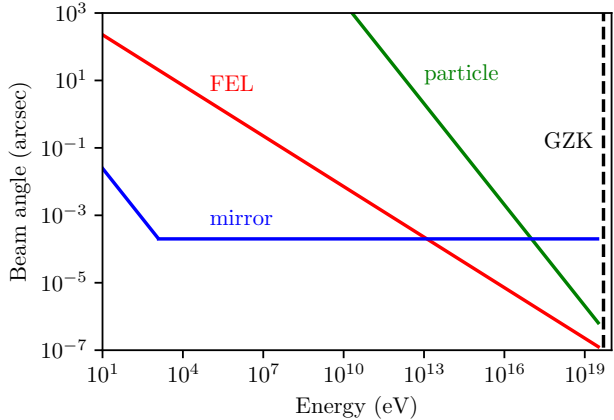


Figure 2. Beam angles of meter-sized photon mirrors, FELs and particle accelerators as a function of particle energy. The mirror cutoff is due to the atomic surface roughness. The GZK cutoff (vertical dashed line) is the Greisen-Zatsepin-Kuzmin limit (Greisen 1966; Zatsepin & Kuz'min 1966) at 5×10^{19} eV ≈ 8 J per photon.

2.3. Focusing with electromagnetic fields instead of physical mirrors

We might then wonder whether it is possible to surpass the limitations of material science by using electromagnetic fields to focus a beam.

An elegant method to directly convert power from electron beams to electromagnetic radiation is the free-electron laser (Madey 1971). The synchrotron radiation generated by a single electron in a beam has a characteristic angular spread of

$$\theta_{\text{electron}} = \frac{1}{\gamma} \approx \frac{0.1}{E \text{ [GeV]}} \text{ [rad]} \quad (3)$$

where γ is the relativistic boost factor of an electron, and E is its energy (ISS Detector Working Group et al. 2009). The beam angle at GeV (TeV, PeV) energies is 6° (21 arcsec, 21 mas). For comparison, the opening angle of diffraction-limited optics is $\theta_{\text{optics}} = 1.22\lambda/D_t$. For $D_t = 1$ m, $\theta_{\text{electron}} = \theta_{\text{optics}}$ at $\lambda = 82$ nm (15 eV), a difference of 7×10^{10} in energy for the same beam width. In other words, focusing particles into a beam of given width requires 7×10^{10} more energy in a particle accelerator (e.g., using TeV particles) compared to a meter-sized mirror (e.g., with 15 eV photons). This limit applies to any particle accelerator, e.g. producing Neutrinos through muon decay. It can be considered as the minimum spread since a particle beam of positive width and angular spread will only increase this angle.

Electron beams can be used to produce photons by passing through the magnetic field of an undulator. Here, the width over which constructive interference is possible is $< 1/\gamma$. Such electrons with rest mass $E_0 = 511$ keV have a relativistic Lorentz factor, e.g. at $E = 6$ GeV (used at the European Synchrotron, Barrett

et al. 1995), $\gamma = E/E_0 \approx 11,742$. An electron beam passing through the magnetic field of an undulator produces photons of $\lambda \approx \lambda_0/2\gamma^2$, where λ_0 is the period length of the undulator (Neil & Merminga 2002). For $\lambda_0 = 28$ mm, we get $\lambda = 0.1$ nm. The width of the photon beam is (Luchini & Motz 1990)

$$\theta_{\text{photon}} = \sqrt{\frac{2\lambda}{L}} \quad (4)$$

where $L = N\lambda_0$ is the length of the machine. This beam is tighter than the electron beam (for the same energy of electrons and photons). It is however wider compared to a classical mirror of the same size, and it scales with the square root of the machine size and the energy, whereas the classical mirror scales proportionally (Figure 2). Consequently, the FEL beam requires TeV energies (at m-sized machines) to achieve the $\theta = 0.2$ mas/ D_t (m) beam width of a meter-sized keV classical mirror. The FEL beam width can be decreased further to 0.01 μ as at the Greisen-Zatsepin-Kuzmin limit (Greisen 1966; Zatsepin & Kuz'min 1966) at 5×10^{19} eV (≈ 8 J per photon, section 5.4), but this is not energy efficient. Spending the same energy on a classical keV beam would deliver more photons to the receiver.

While beam forming efficiency is insufficient to compete with physical devices, wall-plug power efficiency into photons through electron beam deceleration and recycling might ultimately increase to order unity. Literature suggests possible values of 10% (Sprangle et al. 2010), 14% (Emma et al. 2016) or 30% (Sudar et al. 2016). Small (table-top) tunable x-ray lasers might soon be possible through the use of graphene plasmon-based free-electron sources (Wong et al. 2016).

3. ATMOSPHERIC TURBULENCE

The “Cyclops Report”, often dubbed the “SETI bible” (Oliver & Billingham 1971), claimed the superiority of microwaves over other communication methods in the 1960s. One of the reasons was atmospheric turbulence. The report argues (correctly) that “all laser systems suffer the disadvantage of a higher energy per photon than microwave systems (...).” It is then admitted that “this disadvantage is partly compensated by the ease of obtaining narrow beams”, and the following calculation compares the beam widths a 22.5 cm aperture for an IR transmitter to 100 m (and 3,000 m) radio telescopes. The report justifies this choice by “atmospheric turbulence or pointing errors”, which limited beams to arcsec widths.

This was a valid point in the 1960s – but it is less relevant today. The technological progress has been considerable, with adaptive optics soon reaching near-diffraction limited (mas) beam widths (and μ as astrometry) at μ m wavelength for large (39 m) telescopes (Dolaiti et al. 2016), an improvement of 2–3 orders of magnitude. Due to atmospheric absorption for $\lambda < 291$ nm,

X-ray transmitters and receivers need to be placed in space.

4. POINTING ACCURACY

The transmitter's beam needs to be pointed such that the emitted photons arrive at the receiver's position after the photons have traveled the intervening distance. This is in general non-trivial, as beam angles at the optimum wavelength $\lambda \approx \text{nm}$ have small widths of $\theta = 0.2 \text{ mas}/D_t (\text{m})$. As we will see, this beam width is typically small compared to the expected motion of receivers orbiting nearby stars.

4.1. Pointing at planet-based receivers

For illustration, the orbit of a planet in the habitable zone around the nearest star Alpha Centauri A or B has an apparent width of 0.17 arcsec, about $1000 \times$ larger than the beam of a meter-sized telescope. As a result, any transmission attempting to reach distances $\lesssim 1 \text{ kpc}$ must attend carefully to pointing accuracy.

If the receiver is located on a planet sufficiently close that the beam is smaller than its orbit, the transmitting telescope needs to account for the proper motions of the star, plus the orbit of the planet (as noted by [Mankevich & Orlov 2016](#)). Such accuracy for stellar positions and proper motions is possible with current technology. The Gaia mission will achieve astrometry at the μas level ([de Bruijne 2012](#)) in the best cases.

The transmitter must also be able to forecast the receiver's location years or even decades in advance. Forecasts for exoplanet orbits are achievable if they are detected either using the transit or radial velocity method. For example, if an exoplanet is detected via transit, this can be used to predict the timing/duration of its next transit to relatively high accuracy to facilitate follow-up observations, (see e.g. the Transit Predictor Service offered by the NASA Exoplanet Archive²). These follow-up observations are crucial, as transit observations alone are typically insufficient to confirm the planet's full ephemeris (especially the eccentricity). This situation improves as multiple detection methods are brought to bear, and if other planets in the system are detected by e.g. transit timing variations ([Agol & Fabrycky 2017](#)). This allows further constraints on planetary orbits by appealing to arguments based on the orbital stability of the system.

It remains clear that any would-be transmitter attempting to contact a planet-based receiver will begin with some observational constraints on the receiver planet's orbit. These constraints, which may initially be quite loose, will govern strategies for initial communication.

First attempts are likely to have a deliberately larger-than-optimal beam width, to ensure receipt of the signal

in the face of uncertainties regarding the receiver's position when the signal enters their star system. It would seem sensible for any planet-based transmitter to also include details of its own ephemeris, so that a reply from the receiver can be accurately targeted. Ephemerides sharing is likely to be a small but significant component of all interstellar communications.

4.2. Pointing at space-based receivers

As the optimal frequency for interstellar communications is typically absorbed by planetary atmospheres, both transmitter and receiver are likely to be space-based. If the transmitter orbits a planet, then much of the above section applies to this case, with the added need to share the transmitter's orbital parameters as well as the planet's. This also adds a further source of latency - the transmitter/receiver pair are unable to connect when either is occulted by their host planet. Depending on the orbital parameters of both, transmissions will be forced to occur at specific epochs, with well-defined time intervals or windows in which to conduct the conversation.

Another option would be to place the receiver stationary with respect to the star, for example in its gravitational lens (section 6). In this scenario, the transmitter merely needs to point their beam at the star (accounting for its proper motion), rather than forecasting the orbital motion of a planet and its telescope placed on or around it. As noted in [Hippke \(2017b\)](#), tight beams ($\lesssim 3R_\odot$ at the receiver end) should not be pointed at the star directly, but instead at the Einstein ring to maximize the flux in the image plane of the lens. For reference, a $D_t = 1 \text{ m}$ telescope at $\lambda = 1 \text{ nm}$ and $D = 1.3 \text{ pc}$ produces a beam width of $\approx 0.5 R_\odot$. If such a beam were centered on the star, most of the flux would be lost. Therefore, pointing accuracy and proper motion calculations at sub-mas level are required for such a communication. Again, a transmitter choosing to use the SGL would be wise to inform the receiver of this (and details regarding the lens) in its initial communiqués.

5. EXTINCTION

As shown in [Hippke \(2017a\)](#), interstellar extinction prohibits communication near the Lyman limit ([Lyman 1906; Ryter 1996](#)) between $\approx 50 \dots 91.2 \text{ nm}$. This gap separates interstellar communication with low energy ($E < 13.6 \text{ eV}$, $\lambda > 91.2 \text{ nm}$) from that with high energy. The gap widens with increasing distance due to extinction.

5.1. Short distance ($< 100 \text{ pc}$)

For short (pc) communication distances, extinction is negligible (few percent) outside of the gap. For distances up to 100 pc, the optimum frequency in the low energy range remains close to the Lyman limit, at about 100 nm . High energy communication is unaffected and

² <https://exoplanetarchive.ipac.caltech.edu/include/VisibleTransitIntro.html>

placed at the general optimum set by physical mirrors of 1 nm (compare Figure 1).

5.2. Medium distance (100...500 pc)

The gap widens and deepens with distance, resulting in a monotonic increase of the optimum wavelength for low energy communication, from 100 nm at 100 pc distances to 200 nm over 480 pc.

Then, at > 480 pc distances, a considerable step follows (Figure 1) where the optimal low-energy wavelength moves from UV (160 nm) to IR (690 nm). The tipping point is caused by the slope of the extinction function exceeding the focusing advantages. The jitter visible in the optimal IR wavelength comes from infrared absorption bands.

5.3. Large distance (500...8000 pc)

For larger distances, the optimum wavelength increases monotonically. Over kpc, extinction levels of 50% are present at $1 \mu\text{m}$ on the low-energy side, and at 1.5 nm on the high-energy side. For distances of 8 kpc (galactic center), this shifts to $3 \mu\text{m}$ and 0.5 nm , respectively. Therefore, high energy communication near 1 nm wavelength is possible (and optimal) over all relevant galactic distances, perhaps limited in the case of extreme extinction for the innermost few pc of the galactic center.

5.4. Very high frequencies

For very high frequencies, the absorption of MeV and GeV γ -rays in our Galaxy is completely negligible. To absorb a MeV photon with pair production, the target must be another MeV photon. The product of the energies of the two photons must be of order MeV^2 . There are simply not enough MeV (or higher energy) photons traveling in the galaxy to make a significant target. Obviously, the situation is different inside a source or in particular environments, where there is a large density of X- or γ -rays. Therefore, transmittance from the galactic center to earth is near unity for γ -rays up to 10^{12} eV (Moskalenko et al. 2006) or 10^{13} eV (Vernetto & Lipari 2016). Even higher energy photons show a prominent absorption feature between 10^{13} and 10^{17} eV mainly due to interaction with the cosmic microwave background (Zhang et al. 2006). The survival probability over 8 kpc is estimated as 30% at around 10^{15} eV ($= 1 \text{ PeV}$, or $\lambda = 10^{-12} \text{ nm}$) (Vernetto & Lipari 2016). The upper bound for high energy photons is set by the Greisen-Zatsepin-Kuzmin limit (Greisen 1966) at $5 \times 10^{19} \text{ eV}$ ($\approx 8 \text{ J}$) by slowing-interactions of cosmic ray photons with the microwave background radiation over long distances ($\approx 100 \text{ Mpc}$), which has been observationally confirmed (Abraham et al. 2008).

6. LENSING

As discussed in part II of this series (Hippke 2017b), the solar gravitational lens (SGL) enlarges the aperture

(and thus the photon flux) of the receiving telescope by a large factor which is a function of the receiver aperture in the image plane (d_{SGL}), wavelength λ and heliocentric distance z . For a telescope with its center on the axis ($\rho = 0$), the average gain is (Turyshev & Toth 2017, their Eq. 143)

$$\bar{\mu}(z, d_{\text{SGL}}, \lambda) = \frac{4\pi^2}{1 - e^{-4\pi^2 r_g/\lambda}} \frac{r_g}{\lambda} \times \left\{ J_0^2\left(\pi \frac{d_{\text{SGL}}}{\lambda} \sqrt{\frac{2r_g}{z}}\right) + J_1^2\left(\pi \frac{d_{\text{SGL}}}{\lambda} \sqrt{\frac{2r_g}{z}}\right) \right\}, \quad (5)$$

where $r_g = 2GM_{\odot}/c^2 \approx 2,950 \text{ m}$ is the Schwarzschild radius of the sun, and J_x are Bessel functions. This gain is large, for example for $d_{\text{SGL}} = 1 \text{ m}$, $\lambda = 1 \text{ nm}$, $z = 600 \text{ au}$, we get $\bar{\mu} = 2.91 \times 10^9$.

The corresponding circular aperture size $D_{\text{classical}}$ of a telescope outside of the SGL compared to a telescope of size d_{SGL} in the SGL is

$$D_{\text{classical}} = 2\sqrt{\frac{\bar{\mu}d_{\text{SGL}}^2}{4}} = d_{\text{SGL}}\sqrt{\bar{\mu}}. \quad (6)$$

The $d_{\text{SGL}} = 1 \text{ m}$ telescope at $z = 600 \text{ au}$ collects as many photons as a $D_{\text{classical}} = 75.8 \text{ km}$ (kilometer) telescope. The influence of z is within a factor of ≈ 2 between $z_0 = 546 \text{ au}$ and $z = 2,200 \text{ au}$. The difference for a change in wavelength from $\lambda = 1 \text{ nm}$ to $\lambda = 1 \mu\text{m}$ is $\approx 2\%$ and can therefore be neglected.

This gain is so large that despite high coronal noise the achievable data rates are higher by a factor of 10^7 for same size telescopes, as long as the signal is not over-powered by noise. For plausible parameters, the usable regime begins at $P_{\text{t}} > 0.1 \text{ W}$.

7. DATA RATES

In this section, we will calculate the limits on data rates for different distances and parameters, with power from Watt to GW and aperture sizes from $1 \dots 100 \text{ m}$. These parameters cover the capabilities from “Earth 2017” technology with moderate cost (e.g., KW power, meter-sized space telescopes) to advanced, but still plausible “next century” forecasts (e.g., GW power). We assume a conservative capacity of one bit per photon, which corresponds to “Earth 2017” technology. Due to the logarithmic influence of the number of modes on capacity, even very advanced technology will not achieve more than 10 bits per photon in practical cases. Therefore, we can use one bit per photon as an order-of-magnitude argument. As the standard value for wavelength, we use the optimal $\lambda \approx \text{nm}$. With these assumptions, and neglecting extinction, the data rate scales (to within 10%) as

$$\text{DR} \approx d^{-2} D_{\text{t}}^2 D_{\text{r}}^2 P(\text{bits/s}) \quad (7)$$

where d is in pc, D_{t} and D_{r} in m and P in Watt. An important lesson from this relation is that aperture and

power can be traded; a pair of meter-sized telescopes at GW power delivers the same data rate as a pair of 100 m telescopes at 10 W power (or 10 m telescopes at 100 kW power).

A pair of meter-sized probes at Watt power can deliver bits per second per Watt over pc distances. This scales to 10 Gbits/s for $D_t = D_r = 10$ m at MW power. Alternatively, the 1 m Watt-scale probes can be placed in the SGL for a high (10 Mbits/s) data rate. Given nm communication technology, it appears almost trivial to communicate significant data over short interstellar distances.

The DR from the exemplary pair of $D_t = D_r = 10$ m probes at MW power decreases to 100 (1, 0.01 Mbits/s) over distances of 10 (100, 1000 pc). It drops to < 100 bit/s to the galactic center given the added loss from extinction ($S_E \approx 50\%$). Upping the machinery to $D_t = D_r = 100$ m at GW power yields Gbits/s data to the galactic center (7.86 ± 0.18 kpc, Boehle et al. 2016), and 100 kbits/s to Andromeda (752 ± 27 kpc, Riess et al. 2012).

Foreground extinction (galactic and intergalactic) towards Andromeda is surprisingly low at $A(V) = 0.17$ (Schlafly & Finkbeiner 2011), comparable to a distance through the galactic disk of 100 pc. The beam width of the exemplary telescope is $2.5 \mu\text{as}$ at 1 nm, and expands to a width of 1 au at the distance of Andromeda. Such a communication is thus highly selective and targeted at one specific star (or even planet).

The data rate of this link ($D_t = D_r = 100$ m at GW power) drops below kbits/s (bits/s) for distances of 10 (300) Mpc. This advanced, but plausible technology allows for communication throughout the local group of galaxies with reasonable data rates. For reference, transmitting at bits/s delivers 31 Mbits yr^{-1} , sufficient to communicate a substantial book per year.

8. DATA AS A FUNCTION OF MONEY

At first approximation, wavelength can be traded linearly with power and with the squares of the aperture diameters, $\text{DR} \propto \lambda P_t D_t^2 D_r^2$. The relation is linear with the aperture surface area.

It appears plausible that any civilization, even a very advanced, will have non-zero cost for each of these variables. Therefore, ET might strive to maximize bits per time per money. When maximizing this quantity, we can examine the influence of different types of cost functions for wavelength (surface smoothness plus photon production), power and aperture size.

Building the machine (mirror) at a certain size and quality requires fixed (one-off) costs, with additional variable costs (e.g., for maintenance) per bit. The total costs over the finite lifetime of the machine can be attributed per bit. Traditional (filled-aperture) telescope cost functions are progressive for larger sizes, because the supporting structure is to be build in three dimensions to counter gravity, so that the mirror diameter

follows a cubic cost function. Recent technological advances (in the microwave domain) use aperture synthesis combining many smaller dishes, so that the surface area tends more towards a linear, or slightly progressive, cost function. It is unknown if this approach can be extended to X-ray telescopes. Tiled apertures could also be used as multiple coincidence detectors, improving signal-to-noise. In all solutions, the aperture must be sized up as long as the marginal cost for an additional increase in surface area grows beyond a quadratic function. For “Earth 2017” technology, this would be of order meters, or at most tens of meters, in the optical; and hundreds of meters to km for radio.

For the energy production, a linear (proportional) cost function is most plausible, because power plants of a certain capacity can be added as required, with negligible infrastructure overhead. Economies of scale may even result in a regressive cost function. There will be a limit to power because of cooling requirements, which depend on the efficiency, which we neglect here.

Regarding the wavelength, the relevant metric is the surface quality of the machine and its photon production at a constant size and power. As the relation of data rate and frequency is linear, the wavelength should be decreased until the marginal cost for a further improvement increase beyond a linear relation. For example, the baseline might be a $\lambda = 1 \mu\text{m}$ photon production with a laser plus the required ≈ 250 nm (pv) surface smoothness (which is established “Earth 2017” technology). Then, an improvement to $\lambda = 0.5 \mu\text{m}$ and ≈ 125 nm surface smoothness (at the same size and power) must not exceed twice the cost to be beneficial. For “Earth 2017” technology, the optimum is around 193 nm using an ArF (UV) excimer laser and a good mirror, or some other UV to optical laser which is commercially cheap and adequately powerful. This is two orders of magnitude away from the physical optimum.

Earth’s atmosphere absorbs wavelengths < 291 nm so that UV and X-ray communication devices need to be located in space. Currently, this increases costs by orders of magnitude.

In the end the question is whether the physically optimal (\approx nm) wavelength is commercially competitive, or whether e.g. a 2 nm device can be built at less than half the cost, and the money instead invested in more power. This question can not currently be answered. However, we may argue that very advanced technology will offer “cheap” nm-class space-based photon emitters and mirrors. After all, the history of the laser (and other methods) show that technology fills every niche in wavelength over time, at very similar costs.

9. ASTROPHYSICAL NOISE

Noise photons impact the data rate through a reduction of the Holevo capacity, precisely in N_M , which is the number of noise photons per mode. Noise can be instrumental and astrophysical, and we only discuss the latter

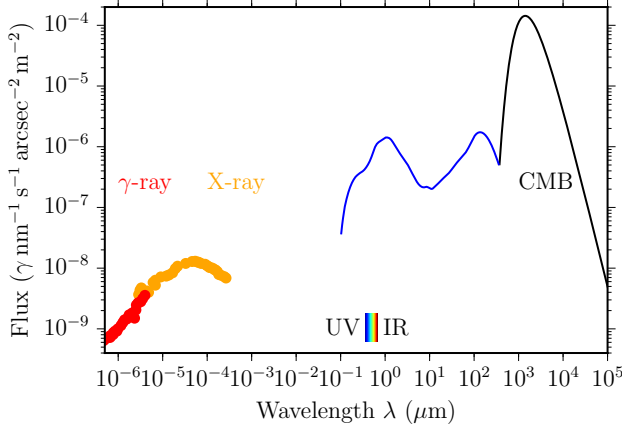


Figure 3. Figure from Hippke (2017a) on the intensity of the sky background after removal of the zodiacal light foreground. Data from Leinert & Mattila (1998); Cooray (2016); Stecker et al. (2016).

here. Astrophysical noise strongly depends on wavelength, with peaks in the optical from nuclear fusion and in the FIR from re-radiated dust (Figure 3). Due to absorption near the Lyman continuum (91.2 nm), the UV/soft X-ray background is unknown. Noise levels for γ - and X-rays between keV and MeV are, within an order of magnitude, $10^{-8} \gamma \text{ nm}^{-1} \text{ s} \text{ arcsec}^{-2} \text{ m}^{-2}$, which is very low. Current technology would result in instrumental noise orders of magnitude higher. X-ray noise levels are two orders of magnitude below optical noise levels. Due to the logarithmic nature of capacity for signal-to-noise levels above unity, noise only impacts the data rate by a factor of a few.

10. DISCUSSION

10.1. Spectral specification of X-ray communication for future SETI searches

The optimal spectrum for maximum data rate connection will have a hard cut at $\lambda > 0.5 \text{ nm}$ due to mirror surface roughness. The bandwidth (towards longer wavelengths) depends on the trade-off between the number of modes (more wavelength channels can encode more bits per photon, favoring large bandwidth) and the beam angle width (which increases due to diffraction with longer wavelength, favoring small bandwidth). As bitrate has a logarithmic relation to the number of modes in realistic cases, and the number of photons scales linear with beamwidth, the bandwidth will be small (< 100%). As a practical example, nanosecond time slots give 10^9 modes per second, so that the monochromatic number of photons can be up to 10^8 s^{-1} before the mode penalty exceeds 1% in bit rate. This means that a GB/s connection will be monochromatic if nanosecond technology is available. Such a connection over pc distances can be done with $D_t = D_r = 10 \text{ m}$ at MW power (section 7).

This work suggests that if we wish to detect transmitters using optimal wavelengths for communication, we should consider carrying out SETI searches in the X-Ray regime, an idea that has been viewed in the past as quite exotic. The first idea to signal with X-ray pulses produced by high-altitude nuclear explosions was considered by Elliot (1973). The idea was later extended to the modulation of X-ray binaries (Corbet 1997, 2016) and dropping matter on neutron stars to produce X-ray flashes (Fabian 1977; Chennamangalam et al. 2015).

X-ray communication is being considered for future deep space missions (Sheng et al. 2014), inter-satellite communication (Mou & Li 2017) and transmission during spacecraft reentry into earth's atmosphere (Li et al. 2017).

We recommend expanding our SETI efforts towards targeted (at us) monochromatic (or narrow band) X-ray emission at 0.5–2 keV energies. Several current X-ray satellites cover this band: Swift (0.2–10 keV), Chandra (0.1–10 keV) and XMM-Newton (0.1–12 keV), while INTEGRAL is only sensitive to higher energies (3 keV–10 MeV). Because of their designs with grazing incidence mirrors, all telescopes have small collecting areas (0.01 m^2 , 0.04 m^2 and 0.45 m^2 for Swift, Chandra and XMM, respectively). With a spectral resolution of $R = 800$ between 0.35–2.5 keV, XMM is well equipped for the proposed narrow-band X-ray signals. As an example, we show the spectrum of Kepler's supernova remnant (SN1604) as observed with XMM-Newton by Cassam-Chenaï et al. (2004) in Figure 4 (left panel). For comparison, synthetic monochromatic and narrow-band spectra are shown in the right panel. As there are thousands of archival X-ray spectra, a dedicated search for such features in existing data can be undertaken (Hippke et al. 2017 in prep.). Compared to the 5.7×10^7 sources visible to XMM over the entire sky (Cappelluti et al. 2007), the number of spectra is small ($< 10^{-4}$ of all detectable sources), but an analysis will already place an upper limit on the number of bright optimally communicating (towards us) X-ray sources; at the moment this number is still unbound.

10.2. Is perfect communication indistinguishable from blackbody radiation?

It has been claimed that any sufficiently advanced technology is entirely indistinguishable from blackbody radiation (Lachmann et al. 2004; Giovannetti et al. 2004b). This is true for the case where an observer is not familiar with the encoding scheme used, and there is zero extinction between transmitter and receiver. For communication near $\lambda \approx \text{nm}$, the blackbody temperature would be $\approx 3 \times 10^6 \text{ K}$, hotter than any stellar surface. Such communication would not be optimal for an isotropic beacon, however, because the energy per photon is unfavorably high compared to radio frequencies.

First of all, it is a misconception that such a perfect blackbody radiation would be indistinguishable from

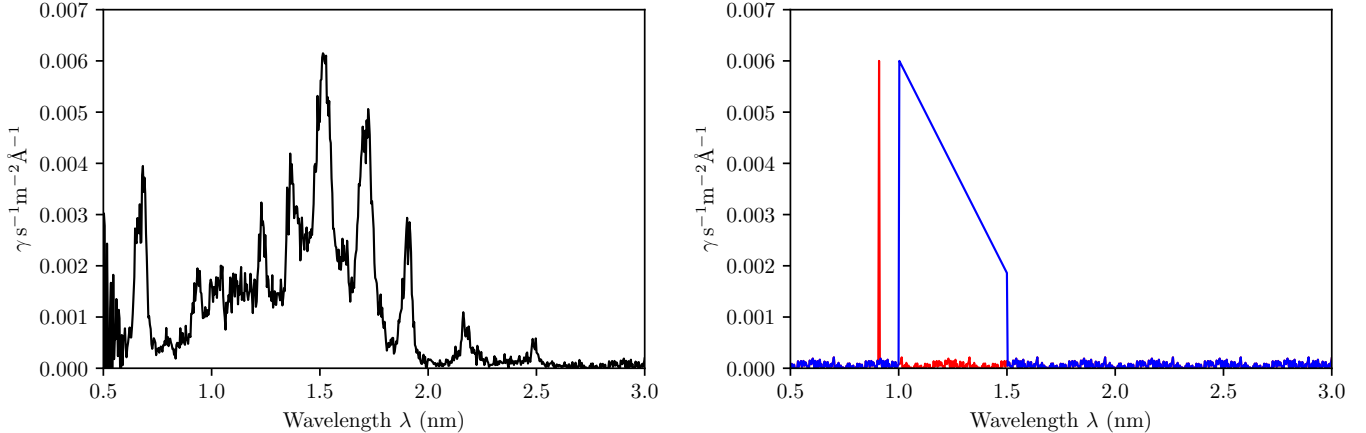


Figure 4. Left: X-ray spectrum taken with XMM-Newton for Kepler's 1604 supernova remnant (Cassam-Chenai et al. 2004). Right: Hypothetical spectra of monochromatic (red) and narrow-band (blue) X-ray signals.

natural sources. Almost all known luminous astrophysical bodies are *not* perfect blackbodies, with the only exception being the Hawking (1975) radiation of a BH³. Even a star originally made of pure hydrogen produces heavier elements through nucleosynthesis, resulting in spectral absorption lines. A recent study used SDSS spectra and found 17 stars out of 789,593 which resemble a perfect blackbody within their measuring uncertainty of 0.01 mag \approx 1% (Suzuki & Fukugita 2017). The authors speculate that these objects are young DB white dwarfs with temperatures around 10000 K. High-resolution high-SNR spectroscopy should reveal some absorption lines; if this is not the case, these objects should be considered prime candidates for targeted OS-ETI. The detection of a perfect blackbody must be extraordinary evidence of artificial origin, as long as it is not a BH or a very young star without nucleosynthesis.

In practical communication, spreading the photons over the total spectrum like a blackbody is inefficient because the interstellar medium is less transparent at some frequencies, and these will be spared in an energy-efficient real-world communication. For example, even the nearest stars are dimmed by many magnitudes near the Lyman limit of 91.2 nm, and one would avoid sending photons in and near this band, because these are (almost entirely) lost. Artificial communication would use hard cuts near such bands, in contrast to a continuous fade for natural sources. A spectrum would show rectangular absorption features instead of a smooth fade.

Also, the choice for a spread spectrum versus narrow band communication has marginal benefits for cases where the number of encoding modes is not the bottleneck. As an order-of-magnitude argument, narrow-band laser communication can readily employ 10^{10} modes by

combining narrowband spectral plus timing encoding. Due to the logarithmic benefits of the number of modes, the number of photons received needs to exceed this order to make a spread spectrum useful – otherwise the capacity (in bits per photon) is virtually identical, so that a blackbody spectrum yields virtually the same number of data bits (per photon and per unit time) as narrowband communication, and only complexity is added.

Receiving 10^{10} photons per unit time (e.g., per second) is a considerable number, comparable to the average (isotropic) luminosity of the nearest stars (10^{26} W) per second per square meter as seen on Earth. To justify the blackbody spread, this number needs to be exceeded by several orders of magnitude. Therefore, such a source would be prominent in the sky.

10.3. Issues with current OSETI searches

If interstellar communication is performed at nm wavelengths (keV energies), traditional optical SETI (300...1000 nm) will not find it, even if it is directed at Earth. Also, Earth's atmosphere is intransparent for photons with $\lambda < 291$ nm, requiring space-based receivers.

The next issue is time resolution. Current OSETI experiments use ns (10^{-9} s) time resolution (Howard et al. 2000; Hanna et al. 2009; Tellis & Marcy 2017). This is not a conscious choice, it is simply a technological limitation. Current (Earth 2017) technology offers superior timing on the transmitter side, compared to the receiver side, by at least 8 orders of magnitude.

Current photon-counting detectors can be relatively fast (timings below 10^{-10} s) and efficient ($> 90\%$) with a low dark count rate (< 1 c.p.s.), but suffer from long (10^{-7} s) reset times (Marsili et al. 2013). Classical photomultiplier tubes offer timings (and reset times) of 10^{-9} s (Dolgoshein et al. 2006).

The shortest possible laser pulse length has decreased by 11 orders of magnitude during the last 50 years, from 100 μ s in the free-running laser of Maiman (1960) to 67

³ The peak wavelength of a BH is close to $16 \times$ its Schwarzschild radius, resulting in a very low power of order 10^{-28} W for a stellar mass BH.

attoseconds (10^{-18} s, Zhao et al. 2012). For a detailed history of the exponential improvements, see Agostini & Di Mauro (2004).

Capacity (in bits per photon) increases with short time slots, and the finite number of astrophysical noise photons per time slot decreases. Therefore, shorter pulses are preferred. If we have the technology to make such pulses, we can assume the same for ETI. So the obvious question is: What will a current OSETI ns receiver see, if the pulses are fs? The answer strongly depends on the flux levels.

To get a feeling for the numbers involved, consider the Harvard SETI's sensitivity threshold of 100 optical photons (with $\lambda = 450 \dots 650$ nm) per square meter, arriving at the telescope in a group within 5 ns (Howard et al. 2004). This translates into the fact that an (average) flux of $< 2 \times 10^{10}$ photons per second per square meter can remain undetected, as long as the clustering appears in unresolved time slots. Even at a meager capacity of 1 bit per photon, the data rate could exceed Gbits/s and remain unnoticed because the encoding remains unresolved. For comparison, the flux from α Cen A is at the same level, $5 \times 10^{10} \gamma \text{ sec}^{-1} \text{ m}^{-2}$ (distance 1.3 pc, Kervella et al. 2016, $L = 1.522L_\odot$). Consequently, an isotropic emitter at pc distance with a flux level of 10^{27} W and fs time slot communication would remain unnoticed, even if the OSETI telescope is aimed directly at it. As we can produce fs pulses today,

it appears likely that ET communication timings are at least as short.

11. CONCLUSION AND OUTLOOK

Optimal directed communication (which maximizes data rates) within the laws of physics converges on $\lambda \approx nm$ wavelengths (keV energies) due to the atomic surface smoothness limit, which cannot efficiently be surpassed with electromagnetic fields. Communication links using this technology can deliver high (Mbits/s, GBits/s) data rates over interstellar distances at moderate apertures and power. We may argue that mature civilizations would not use inefficient technologies such as burning kerosene or sending microwaves, optical or IR photons. Instead, we may assume that ET have developed cost-efficient technology required for the optimum communication, and have established such communication links. For these tight communication beams, the chance of a random intercept at Earth is very small (Forgan 2014), so that classical SETI is in vain. This topic will be covered in a subsequent part of this series.

Acknowledgments. The authors are thankful to Silvia Vernetto for explanations on γ -ray absorption, to Cris More for an exchange on the similarity of information-efficient communication to black-body radiation, to Zachary Manchester and René Heller for helpful discussions, and to the Breakthrough Initiatives for an invitation to the Breakthrough Discuss 2017 conference at Stanford University.

REFERENCES

Abraham, J., Abreu, P., Aglietta, M., et al. 2008, *Physical Review Letters*, 101, 061101

Agol, E., & Fabrycky, D. 2017, ArXiv e-prints, [arXiv:1706.09849 \[astro-ph.EP\]](https://arxiv.org/abs/1706.09849)

Agostini, P., & Di Mauro, L. F. 2004, *Reports on Progress in Physics*, 67, 813

Aller, L. H. 1959, *PASP*, 71, 324

Aristov, V. V., & Shabel'nikov, L. G. 2008, *Physics Uspekhi*, 51, 57

Barrett, R., Baruchel, J., Hartwig, J., & Zontone, F. 1995, *Journal of Physics D Applied Physics*, 28, A250

Barstow, M. A., & Holberg, J. B. 2007, Extreme Ultraviolet Astronomy

Bean, R. J., Aquila, A., Samoylova, L., & Mancuso, A. P. 2016, *Journal of Optics*, 18, 074011

Boehle, A., Ghez, A. M., Schödel, R., et al. 2016, *ApJ*, 830, 17

Bohr, N. 1913, *Philosophical Magazine*, 26, 476

Cappelluti, N., Hasinger, G., Brusa, M., et al. 2007, ArXiv e-prints, [arXiv:0704.2293](https://arxiv.org/abs/0704.2293)

Cassam-Chenaï, G., Decourchelle, A., Ballet, J., et al. 2004, *A&A*, 414, 545

Chennamangalam, J., Siemion, A. P. V., Lorimer, D. R., & Werthimer, D. 2015, *NewA*, 34, 245

Cocconi, G., & Morrison, P. 1959, *Nature*, 184, 844

Cooray, A. 2016, *Royal Society Open Science*, 3, 150555

Corbet, R. H. D. 1997, *Journal of the British Interplanetary Society*, 50, 253

—. 2016, ArXiv e-prints, [arXiv:1609.00330 \[astro-ph.HE\]](https://arxiv.org/abs/1609.00330)

Crowe, M. 1999, *The Extraterrestrial Life Debate, 1750-1900* (Dover Publications)

Danjon, A., & Couder, A. 1935, *Lunettes et telescopes - Theorie, conditions d'emploi, description, reglage*

de Bruijne, J. H. J. 2012, *Ap&SS*, 341, 31

Diolaiti, E., Ciliegi, P., Abicca, R., et al. 2016, in *Proc. SPIE, Vol. 9909, Adaptive Optics Systems V*, 99092D

Dolgoshein, B., Balagura, V., Buzhan, P., et al. 2006, *Nuclear Instruments and Methods in Physics Research A*, 563, 368

Elliot, J. L. 1973, X-ray pulses for interstellar communication, ed. C. Sagan, 398

Emma, C., Fang, K., Wu, J., & Pellegrini, C. 2016, *Physical Review Special Topics Accelerators and Beams*, **19**, 020705

Fabian, A. C. 1977, *Journal of the British Interplanetary Society*, **30**, 112

Forgan, D. H. 2014, *Journal of the British Interplanetary Society*, **67**, 232

Gingerich, O. 2003, Interview of Philip Morrison by Owen Gingerich (American Institute of Physics, College Park, MD USA)

Giovannetti, V., García-Patrón, R., Cerf, N. J., & Holevo, A. S. 2014, *Nature Photonics*, **8**, 796

Giovannetti, V., Guha, S., Lloyd, S., Maccone, L., & Shapiro, J. H. 2004a, *PhRvA*, **70**, 032315

Giovannetti, V., Lloyd, S., Maccone, L., & Shapiro, J. H. 2004b, *PhRvA*, **69**, 052310

Greisen, K. 1966, *Physical Review Letters*, **16**, 748

Hanna, D. S., Ball, J., Covault, C. E., et al. 2009, *Astrobiology*, **9**, 345

Hawking, S. W. 1975, *Communications in Mathematical Physics*, **43**, 199

Hippke, M. 2017a, ArXiv e-prints, [arXiv:1706.03795 \[astro-ph.IM\]](https://arxiv.org/abs/1706.03795)

—. 2017b, ArXiv e-prints, [arXiv:1706.05570 \[astro-ph.EP\]](https://arxiv.org/abs/1706.05570)

Holevo, A. S. 1973, Problemy Peredachi Informatsii, **9**, 3

Howard, A., Horowitz, P., Coldwell, C., et al. 2000, in *Astronomical Society of the Pacific Conference Series*, Vol. 213, *Bioastronomy 99*, ed. G. Lemarchand & K. Meech

Howard, A. W., Horowitz, P., Wilkinson, D. T., et al. 2004, *ApJ*, **613**, 1270

ISS Detector Working Group, Abe, T., Aihara, H., et al. 2009, *Journal of Instrumentation*, **4**, T05001

Kervella, P., Mignard, F., Mérand, A., & Thévenin, F. 2016, *A&A*, **594**, A107

Kirkpatrick, P., & Baez, A. V. 1948, *Journal of the Optical Society of America* (1917-1983), **38**, 766

Lachmann, M., Newman, M. E. J., & Moore, C. 2004, *American Journal of Physics*, **72**, 1290

Leinert, C., & Mattila, K. 1998, in *Astronomical Society of the Pacific Conference Series*, Vol. 139, *Preserving The Astronomical Windows*, ed. S. Isobe & T. Hirayama, 17

Li, H., Tang, X., Hang, S., Liu, Y., & Chen, D. 2017, *Journal of Applied Physics*, **121**, 123101

Lowell, P. 1904, *Lowell Observatory Bulletin*, **1**, 59

Luchini, P., & Motz, H. 1990, *Undulators and free-electron lasers*, International series of monographs on physics (Clarendon Press)

Lyman, T. 1906, *ApJ*, **23**, 181

Madey, J. M. J. 1971, *Journal of Applied Physics*, **42**, 1906

Maiman, T. H. 1960, *Nature*, **187**, 493

Mankevich, S. K., & Orlov, E. P. 2016, *Quantum Electronics*, **46**, 966

Marsili, F., Verma, V. B., Stern, J. A., et al. 2013, *Nature Photonics*, **7**, 210

Moskalenko, I. V., Porter, T. A., & Strong, A. W. 2006, *ApJL*, **640**, L155

Mou, H., & Li, B.-q. 2017, *Proceedings of the SPIE*, Volume 10256, id. 102561W [NUMPAGES_6]/NUMPAGES_6 pp. (2017)., **256**, 102561W

Neil, G. R., & Merminga, L. 2002, *Reviews of Modern Physics*, **74**, 685

Oliver, B. M., & Billingham, J., eds. 1971, *Project Cyclops: A Design Study of a System for Detecting Extraterrestrial Intelligent Life*

Pickering, W. 1909, *Cambridge Chronicle*, May 1, 7

Rayleigh, L. 1879, *Philosophical Magazine Series* **5**, **8**, 261

Riess, A. G., Fliri, J., & Valls-Gabaud, D. 2012, *ApJ*, **745**, 156

Ryter, C. E. 1996, *Ap&SS*, **236**, 285

Schiaparelli, G. V. 1878, *Memorie della Societa Degli Spettroscopisti Italiani*, **7**, B21

Schlafly, E. F., & Finkbeiner, D. P. 2011, *ApJ*, **737**, 103

Schwartz, R. N., & Townes, C. H. 1961, *Nature*, **190**, 205

Sheng, L.-z., Zhao, B.-s., & Liu, Y.-a. 2014, in *Proc. SPIE*, Vol. 9207, *Advances in X-Ray/EUV Optics and Components IX*, 920716

Siewert, F., Buchheim, J., Boutet, S., et al. 2012, *Optics Express*, **20**, 4525

Singh, M., & Braat, J. J. M. 2000, *ApOpt*, **39**, 2189

Smith, W. J. 2008, *Modern Optical Engineering: The Design of Optical Systems*, Fourth Edition (The McGraw-Hill Companies)

Sprangle, P., Penano, J., Hafizi, B., & Ben-Zvi, I. 2010, *IEEE Journal of Quantum Electronics*, **46**, 1135

Stecker, F. W., Scully, S. T., & Malkan, M. A. 2016, *ApJ*, **827**, 6

Strehl, K. 1894, *Theorie des Fernrohrs. Auf Grund der Beugung des Lichts. 1 Teil.*

Sudar, N., Musumeci, P., Duris, J., et al. 2016, *Physical Review Letters*, **117**, 174801

Suzuki, N., & Fukugita, M. 2017, ArXiv e-prints, [arXiv:1711.01122 \[astro-ph.SR\]](https://arxiv.org/abs/1711.01122)

Suzuki, Y. 2004, *Japanese Journal of Applied Physics*, **43**, 7311

Tellis, N. K., & Marcy, G. W. 2017, *AJ*, **153**, 251

Tesla, N. 1901, *Collier's Weekly* **26**, Feb 9, 1, 4

Texereau, J. 1984, How to make a telescope adapted from the French

Tsuru, T., Tosaka, A., Sakai, Y., & Yamamoto, M. 2009, in *Journal of Physics Conference Series*, Vol. 186, *Journal of Physics Conference Series*, 012077

Turyshev, S. G., & Toth, V. T. 2017, ArXiv e-prints, [arXiv:1704.06824 \[gr-qc\]](https://arxiv.org/abs/1704.06824)

Van Tran, J. 1992, *Frontiers of Life, Rencontres de Blois* (Editions Frontieres)

Vernetto, S., & Lipari, P. 2016, *PhRvD*, 94, 063009

Weisskopf, M. C. 2012, *Optical Engineering*, 51, 011013

Wilms, J., Allen, A., & McCray, R. 2000, *ApJ*, 542, 914

Wong, L. J., Kaminer, I., Ilic, O., Joannopoulos, J. D., & Soljačić, M. 2016, *Nature Photonics*, 10, 46

Yamamoto, M. 2001, *Nuclear Instruments and Methods in Physics Research A*, 467, 1282

Yu, J., Namba, Y., Ngoi, B. K., & Zhong, Z. 1999, in Proc. 14th ASPE Annual Meeting, Monterey, 368

Zatsepin, G. T., & Kuz'min, V. A. 1966, *Soviet Journal of Experimental and Theoretical Physics Letters*, 4, 78

Zhang, J.-L., Bi, X.-J., & Hu, H.-B. 2006, *A&A*, 449, 641

Zhao, K., Zhang, Q., Chini, M., et al. 2012, *Optics Letters*, 37, 3891